Axonal oscillations in developing mammalian nerve axons

Shangyou Zeng and Peter Jung
Department of Physics and Astronomy and Quantitative Biology Institute, Ohio University, Athens, Ohio 45701, USA
(Received 7 July 2004; published 25 January 2005)

We study neuronal spike propagation in a developing myelinated axon in various stages of its development through detailed computational modeling. Recently, a form of bursting (*axonal bursting*), has been reported in axons in developing nerves in the absence of potassium channels. We present a computational study using a detailed model for a myelinated nerve in development to explore under what circumstances such an effect can be expected. It is shown that axonal oscillation may be caused by backfiring between the nodes of Ranvier or through backfiring from internodal sodium channels or by reducing the thickness of the myelin wrapping the axon between the nodes of Ranvier.

DOI: 10.1103/PhysRevE.71.011910 PACS number(s): 87.19.La, 87.10.+e

I. INTRODUCTION

An important requirement for the successful evolution to large body sizes of organisms is the stable, efficient, and fast propagation of action potentials across the long axons of the peripheral nervous system. An elegant solution of this problem is the development of the myelinated axon, where the sodium channels are concentrated at the nodes of Ranvier, separated by segments sheathed with myelin. The myelin sheath is a high resistance, low capacitance barrier for the axonal membrane and provides the basis for fast propagation of action potentials. The nodes of Ranvier are distributed along the axon where the myelin is interrupted at distances ranging from 50 μm to 1000 μm for different nerves. These spatial axonal domains differ dramatically from the internodal axonal regions. Voltage-dependent sodium channels can be found in the nodes of Ranvier at a much larger density (approximately $2000/\mu m^2$ [1]) than in the internodal region [2–5] (of the order $10/\mu m^2$). Furthermore, the capacitance of the nodes of Ranvier is higher than that of internodal region. Voltage-dependent potassium channels are excluded from nodes of Ranvier [6]; they are clustered beneath the myelin sheaths in regions adjacent to paranodes, called juxtaparanodes [2,7].

Potassium ion channels play an important role in the modulation of excitability [1]. In their pioneering work on neuronal excitability, Hodgkin and Huxley [8] demonstrated that potassium ion channels play an important role in the repolarization of action potential in the squid giant axon. Blockage of internodal potassium ion channels in young dorsal roots [9] and regenerating rat nerve fibers [10] results in a bursting activity triggered by a single impulse. Vabnick *et al.* [11] demonstrated that internodal potassium ion channels prevent bursting activity in the developing sciatic nerve of rat. In contrast, blockage of internodal potassium ion channels does not affect the spike waveform and firing properties of normal mature sciatic nerve fibers [10].

Although sodium ion channels clustered in nodes of Ranvier provide the physiological basis for saltatory conduction, the function of internodal potassium ion channels remains unclear. There are two suggestions about the function of internodal potassium ion channels. One suggestion is that they stabilize the paranodal axolemma against nodal backfiring after a single impulse [2]. The other suggestion is that the function of internodal potassium ion channels is to maintain a resting potential under the myelin [12,13]. In this paper, we use a computational model for a developing mammalian axon to explore the role of the spatial distribution of potassium channels with regard to reliability and speed of action potential propagation. Our main result is that the observed configuration of juxtaparanodal concentration of potassium channels optimizes speed and reliability of action potential propagation during the development of the axon.

II. THE MODEL

A. Hodgkin-Huxley equations

The electrical potential of nerve membranes was first quantitatively described in terms of a mathematical model by Hodgkin and Huxley [8]. Accordingly, the time evolution of the electrical potential across the membrane is given by the following equations

$$c_m \frac{dV}{dt} = g_{\mathrm{Na}}(V_{\mathrm{Na}} - V) + g_{\mathrm{K}}(V_{\mathrm{K}} - V) + g_{\mathrm{leak}}(V_{\mathrm{leak}} - V) + I, \tag{1}$$

where c_m denotes the specific capacitance (capacitance per area) of the nerve membrane, and g_{Na}, g_{K} and g_{leak} the conductance of the sodium channels, potassium channels and leakage system, respectively. The voltages V_{Na}, V_{K} and V_{leak} denote the sodium, potassium and leakage reversal potentials and I is injected current. While the leakage conductance g_{leak} is a constant, the sodium and potassium conductance, g_{Na} and g_{K}, are voltage (V) dependent, i.e.,

$$g_{\mathrm{Na}} = \overline{g}_{\mathrm{Na}} m^3(V,t)[h(V,t)],$$

$$g_{\mathrm{K}} = \overline{g}_{\mathrm{K}} n^4(V,t), \tag{2}$$

where $\overline{g}_{\mathrm{Na}}$ denotes the maximal sodium conductance (all sodium channels open), and $\overline{g}_{\mathrm{K}}$ the maximal potassium conductance (all potassium channels open). The gating variables m, n and h, with $0 < m, n, h < 1$ are voltage dependent, and governed by the set of linear equations

$$\frac{dn}{dt} = -[\alpha_n(V) + \beta_n(V)]n + \alpha_n(V),$$

$$\frac{dm}{dt} = -[\alpha_m(V) + \beta_m(V)]m + \alpha_m(V),$$

$$\frac{dh}{dt} = -[\alpha_h(V) + \beta_h(V)]h + \alpha_h(V), \tag{3}$$

with the rates

$$\alpha_n(V) = \frac{0.0462(V+83.2)}{1-e^{-(V+83.2)/1.1}},$$

$$\beta_n(V) = \frac{-0.0824(V+66)}{1-e^{(V+66)/10.5}},$$

$$\alpha_m(V) = \frac{6.57(V+20.4)}{1-e^{-(V+20.4)/10.3}},$$

$$\beta_m(V) = \frac{-0.304(V+25.7)}{1-e^{(V+25.7)/9.16}},$$

$$\alpha_h(V) = \frac{-0.34(V+114)}{1-e^{(V+114)/11}},$$

$$\beta_h(V) = \frac{12.6}{1+e^{-(V+31.8)/13.4}}. \tag{4}$$

The voltages V in Eq. (4) are measured in millivolts.

B. Compartmental model for the axon

In order to describe the spatial and temporal evolution of the action potential along the heterogeneous axon, a spatially explicit model of the axon is needed. For a homogeneous axon, the cable equation for a one-dimensional axon (along x coordinate) is given by (see, e.g., in [14]),

$$c_m \frac{\partial V(x,t)}{dt} + i_{\text{ion}}(V) = \frac{d}{4\rho_a}\frac{\partial^2 V}{\partial x^2}, \tag{5}$$

where ρ_a denotes the axoplasmic resistivity, d the diameter of the axon, and c_m the membrane capacitance per area. The ionic current sources

$$i_{\text{ion}} = g_{\text{Na}}(V - V_{\text{Na}}) + g_{\text{K}}(V - V_{\text{K}}) + g_{\text{leak}}(V - V_{\text{leak}}) \tag{6}$$

are given by the Hodgkin-Huxley model described in the previous section. Multiplying Eq. (5) with a characteristic resistance R, it becomes clear that $\tau_m = RC$ determines the typical time scale of the cable equation and $\sqrt{Rd/\rho_a}$ the typical length-scale of the cable equation. Dimensional arguments thus yield to the propagation speed of an action potential $u \propto d^{1/2}/c_m$. Thus increasing the capacitance c_m of the membrane will decrease the speed of the action potential while increasing the diameter of the axon will increase the speed of the action potential.

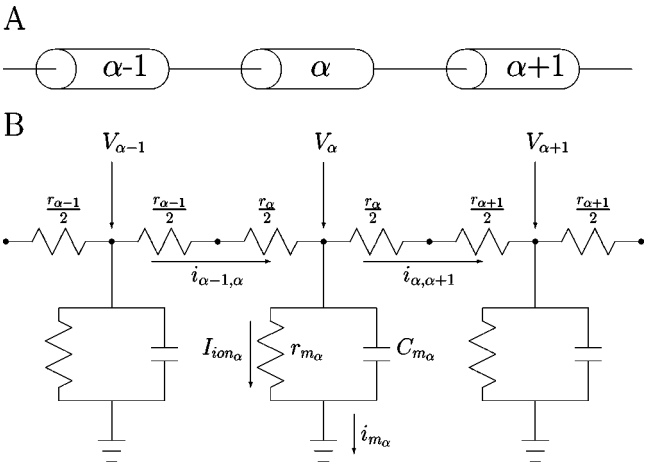

FIG. 1. (a) A chain of three cylindrical compartments that are sufficiently short to be considered isopotential. (b) Equivalent circuit for a compartmental model of a chain of three successive small cylindrical compartments of passive axonal membrane.

The compartmental model replaces the continuous partial differential equation of the cable model [Eq. (5)] by a set of N ordinary differential equations. There are two key advantages of this model. First, the flexibility of the compartmental model ensures that this model can embody the structure and physiological differences of the specific dendrite. Second, the compartmental model can be implemented directly on a computer. In the compartmental model, an unbranched region of an axon is divided into a number of contiguous compartments [15]. Each compartment is small enough to be considered as isopotential. Then the differences in physical properties and potential only occur between two nearby compartments rather than in one compartment [16,17].

We consider an unbranched, cylindrical region of a passive axon, divided into three linked compartments. A linked chain of equivalent electrical circuits illustrating this region is shown in Fig. 1(a). These compartments are represented by the equivalent circuit of Fig. 1(b). As shown in Fig. 1(b), the circuit of each compartment consists of a capacitor in parallel with a resistor. Each compartment α is joined to its immediate neighbors by junctional resistors $r_{\alpha-1,\alpha}$ and $r_{\alpha,\alpha+1}$. If the cylindrical compartment α has the uniform diameter d and length l_α, the membrane capacitance C_{m_α} and resistance r_{m_α} of the αth compartment are given by

$$C_{m_\alpha} = c_{m_\alpha} l_\alpha \pi d,$$

$$r_{\alpha,\alpha'} = \frac{r_\alpha}{2} + \frac{r_{\alpha'}}{2} = \frac{2r_{m_\alpha} l_\alpha + 2r_{m_{\alpha'}} l_{\alpha'}}{\pi d^2}, \tag{7}$$

where c_{m_α} and g_α are the membrane capacitance and conductance per unit area, respectively.

The compartmental model is represented by a set of ordinary differential equations. Each equation is derived from Kirchhoff's current law. In each compartment, α, the net current through the membrane, i_α, must equal to the longitudinal current that enters that compartment minus the longitudinal current that leaves it. If the αth compartment lies

between the $(\alpha-1)$th and the $(\alpha+1)$th compartments, the membrane current of compartment α is given by

$$i_{m_\alpha} = i_{\alpha-1,\alpha} - i_{\alpha,\alpha+1}, \tag{8}$$

where $i_{\alpha-1,\alpha}$ is the current that flows from compartment $\alpha-1$ to compartment α and $i_{\alpha,\alpha+1}$ is the current that flows from compartment α to $\alpha+1$. The membrane current is the sum of the capacitance (charging) current and the net ionic current (i_{ion}) that flows through the transmembrane resistance. For the compartment α, the membrane current can be expressed as

$$i_{m_\alpha} = C_{m_\alpha}\frac{dV_\alpha}{dt} + i_{\text{ion}_\alpha}, \tag{9}$$

where V_α is the membrane potential measured with respect to the resting potential. The longitudinal current is the voltage gradient between two nearby compartments divided by the axial resistance between the two compartments. Thus combining Eq. (8) and Eq. (9), we can get the following equations

$$i_{m_\alpha} = C_{m_\alpha}\frac{dV_\alpha}{dt} + i_{\text{ion}_\alpha} = \frac{V_{\alpha-1}-V_\alpha}{r_{\alpha-1,\alpha}} - \frac{V_\alpha - V_{\alpha+1}}{r_{\alpha,\alpha+1}} \tag{10}$$

or

$$i_{m_\alpha} = C_{m_\alpha}\frac{dV_\alpha}{dt} + i_{\text{ion}_\alpha} = (V_{\alpha-1}-V_\alpha)g_{\alpha-1,\alpha} - (V_\alpha - V_{\alpha+1})g_{\alpha,\alpha+1}, \tag{11}$$

where $g_{\alpha-1,\alpha}=1/r_{\alpha-1,\alpha}$ is the axial conductance between the $(\alpha-1)$th compartment and the αth compartment. For the first compartment in a chain, only the second term for the longitudinal current appears on the right-hand side of the equations; for the last compartment in a chain, only the first term for the longitudinal current appears on the right-hand side of the equations.

Inserting the explicit expression for the ionic transmembrane currents (for all compartments α)

$$i_{m_\alpha} = C_{m_\alpha}\frac{dV_\alpha}{dt} + g_{\text{leak},\alpha}(V_\alpha - V_{\text{leak},\alpha}) + g_{\text{Na},\alpha}(V_\alpha - V_{\text{Na},\alpha}) + g_{\text{K},\alpha}(V_\alpha - V_{\text{K},\alpha}) \tag{12}$$

into Eq. (11), one finds

$$C_m\frac{dV_\alpha}{dt} = g_{\alpha-1,\alpha}V_{\alpha-1} + g_{\alpha,\alpha+1}V_{\alpha+1} - (g_{\text{leak},\alpha} + g_{\text{Na},\alpha} + g_{\text{K},\alpha} + g_{\alpha-1,\alpha} + g_{\alpha,\alpha+1})V_\alpha + g_{\text{leak},\alpha}V_{\text{leak},\alpha} + g_{\text{Na},\alpha}V_{\text{Na},\alpha} + g_{\text{K},\alpha}V_{\text{K},\alpha}. \tag{13}$$

We consider two nodes of Ranvier connected by an axon. There are 10 compartments between two successive nodes [18]. The present model provides an explicit representation of the node of Ranvier, the myelin attachment compartments (MYSA), the paranode main compartments (FLUT) and the internodal compartments (STIN). The geometric structure of the cable model is shown in Fig. 2. Sodium ion channels exist in a high density in the node of Ranvier, and a very low density in the internodal region. Potassium ion channels only exist in the juxtaparanodal region. The nodes consists of a parallel combination of the nonlinear sodium conductance, the leakage conductance and the membrane capacitance. The internodal region consist of a parallel combination of the nonlinear sodium conductance, nonlinear potassium conductance, the leakage conductance, and the membrane capacitance. The parameters of the cable model are listed in Table I.

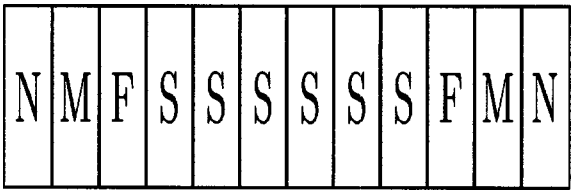

FIG. 2. The cable model with 10 internodal compartments. Each internodal section of the model consists of 2 myelin attachment compartment (MYSA, M in the figure), 2 paranode main compartment (FLUT, F in the figure) and 6 internodal compartments (STIN, S in the figure). N denotes the nodal compartment.

III. RESULTS

A. Oscillation activity of myelinated axon in development by blockage of internodal potassium channels

Myelin isolates the cytoplasmic core of the axon from the extracellular environment, and provides low internodal capacitance and high transverse resistance for the membrane [19]. During the development of the axon, the thickness of the myelin increases and thus, the internodal capacitance and leakage currents decrease [20]. Due to the segregation of sodium ion channels and the isolating effect of myelin, the conductance of internodal sodium ion channels will also decrease in development [4]. In order to simulate action poten-

TABLE I. Axonal parameters.

Axon diameter	5 μm
Axoplasmic resistivity	70 Ω cm
Na^+ reversal potential	50 mV
K^+ reversal potential	−90 mV
Leakage reversal potential	−80 mV
Nodal membrane capacitance	2 μF/cm^2
Na^+ conductance in nodal region	800 mS/cm^2
Nodal leakage current conductance	8 mS/cm^2
Nodal length	1 μm
Internodal membrane capacitance	0.005–0.03 μF/cm^2
Internodal Na^+ conductance	0.5–3 μF/cm^2
Internodal leakage current conductance	0.005–0.03 mS/cm^2
MYSA, STIN K^+ conductance	0–10 mS/cm^2
FLUT K^+ conductance	0–86.5 mS/cm^2
MYSA length	3 μm
FLUT length	20 μm
STIN length	50 μm

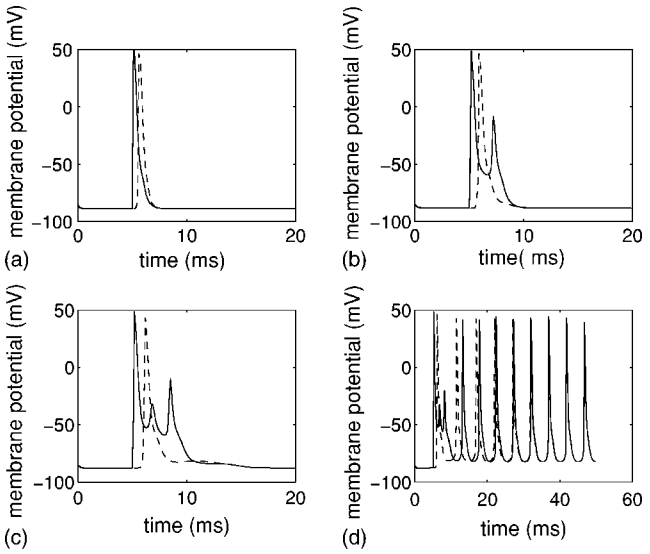

FIG. 3. Action potentials of two connected nodes without juxtaparanodal and internodal potassium channels. The solid lines represent the action potential of node one and the dashed lines denote the action potentials of node two. Current is injected into node one to evoke an action potential. (a) $g_{\mathrm{Na}_i}=0.5$ mS/cm^2; $g_{\mathrm{leak}_i}=0.005$ mS/cm^2; $c_{m_i}=0.005$ μF/cm^2. (b) $g_{\mathrm{Na}_i}=1$ mS/cm^2; $g_{\mathrm{leak}_i}=0.01$ mS/cm^2; $c_{m_i}=0.01$ μF/cm^2. (c) $g_{\mathrm{Na}_i}=2$ mS/cm^2; $g_{\mathrm{leak}_i}=0.02$ mS/cm^2; $c_{m_i}=0.02$ μF/cm^2. (d) $g_{\mathrm{Na}_i}=3$ mS/cm^2; $g_{\mathrm{leak}_i}=0.03$ mS/cm^2; $c_{m_i}=0.03$ μF/cm^2.

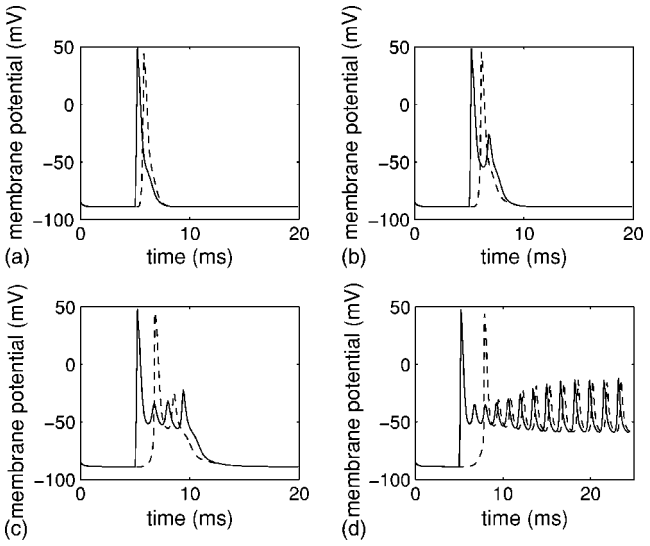

FIG. 4. Action potentials of two connected nodes without juxtaparanodal potassium ion channels. The solid line denotes the action potential of node one, while the dashed line represents the action potential of node two. Stimuli current is injected in node one. The parameters are $g_{\mathrm{Na}_i}=0.5$ mS/cm^2, $g_{\mathrm{leak}_i}=0.005$ mS/cm^2, $c_{m_i}=0.005$ μF/cm^2 (a), $c_{m_i}=0.01$ μF/cm^2 (b), $c_{m_i}=0.02$ μF/cm^2 (c), and $c_{m_i}=0.03$ μF/cm^2 (d).

tials in development, we increase the internodal capacitance, leakage conductance and internodal sodium channel conductance proportionally. In order to determine the effect of juxtaparanodal potassium ion channels, we first set the potassium conductance zero everywhere.

We simulate four groups of data. In the first group, the conductance of internodal sodium ion channels $g_{\mathrm{Na}_i}=0.5$ mS/cm^2, the conductance of internodal leakage current $g_{\mathrm{leak}_i}=0.005$ mS/cm^2 and the capacitance of the internodal membrane $c_{m_i}=0.005$ μF/cm^2. In the second group, $g_{\mathrm{Na}_i}=1$ mS/cm^2, $g_{\mathrm{leak}_i}=0.01$ mS/cm^2 and $c_{m_i}=0.01$ μF/cm^2. In the third group, $g_{\mathrm{Na}_i}=2$ mS/cm^2, $g_{\mathrm{leak}_i}=0.02$ mS/cm^2 and $c_{m_i}=0.02$ μF/cm^2. In the fourth group, $g_{\mathrm{Na}_i}=3$ mS/cm^2, $g_{\mathrm{leak}_i}=0.03$ mS/cm^2 and $c_{m_i}=0.03$ μF/cm^2. External current is injected in node one to evoke an action potential. Action potentials in the four groups of data are plotted in Fig. 3. In the first group, the values of g_{Na_i}, g_{leak_i} and c_{m_i} are very small, corresponding to a more mature axon. As shown in Fig. 3(a), the action potential evoked in node one (solid line) by an external current, propagates along the axon to node two (dashed line), where it evokes another action potential. This behavior is consistent with the observation that blockage of internodal potassium ion channels does not affect the spike waveform and firing properties of normal mature axons [10]. As shown in Figs. 3(b)–3(d), the shape of the action potentials changes gradually when the values of the internodal sodium conductance g_{Na_i}, leakage conductance g_{leak_i} and internodal capacitance c_{m_i} are increased, corresponding to an axon in an earlier stage of development. Consistent with observations in developing axons [9,10] we observe multiple spikes in nodes one and two in the absence of potassium channels. In Fig. 3(c), bursting activity can be observed; in Fig. 3(d), tonic spiking can be observed. In the following section we discuss what parameter changes can cause these oscillations.

B. Effects of parameters of internodal membrane on oscillation activity

In order to determine the effect of each parameter, we only change one parameter value, and keep the values of other parameters constant. First, we test the effect of leakage conductance. At constant values of $g_{\mathrm{Na}_i}=0.5$ mS/cm^2, and $c_{m_i}=0.005$ μF/cm^2, we change the value of g_{leak_i} from 0.005 mS/cm^2 to 0.03 mS/cm^2. An external current pulse is injected into node one to evoke an action potential. Simulation results (not shown in the paper) show that the leakage current does not change the shape of action potentials. Thus the leakage current is not the source of oscillation activity.

Next we investigate the effect of the internodal membrane capacitance. At constant values of $g_{\mathrm{Na}_i}=0.5$ mS/cm^2 and $g_{\mathrm{leak}_i}=0.005$ mS/cm^2, we change the value of c_{m_i} from 0.005 μF/cm^2 to 0.03 μF/cm^2. An external current pulse is injected into node one to evoke an action potential. The subsequent membrane potentials at both nodes are plotted in Fig. 4. As shown in Fig. 4, the shape of the action potentials—similar as in Fig. 3—change gradually as the internodal membrane capacitance is increasing. When the capacitance increases beyond a certain value, the axon can respond with multiple spikes (at each node) to a single action potential. For large enough capacitance, tonic oscillation occurs. Thus, a relative big value of internodal membrane capacitance in development is a source of axonal oscillation if

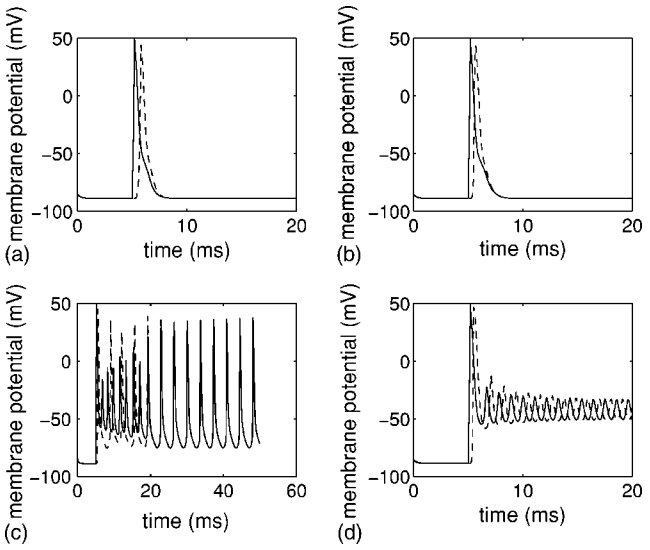

FIG. 5. Action potentials of two connected nodes without juxtaparanodal potassium ion channels. The solid line depicts the action potentials of node one and the dashed line represents the action potential of node two. An electrical current pulse is injected into node one to evoke an action potential. The parameter values are $g_{\mathrm{leak}_i}=0.005$ mS/cm^2, $c_{m_i}=0.005$ μF/cm^2, $g_{\mathrm{Na}_i}=0.5$ mS/cm^2 (a), $g_{\mathrm{Na}_i}=1$ mS/cm^2 (b), $g_{\mathrm{Na}_i}=2$ mS/cm^2 (c), and $g_{\mathrm{Na}_i}=3$ mS/cm^2 (d).

the internodal potassium ion channels are blocked.

A simple theory can predict the onset of axonal oscillations. Given the refractory time of a node of about $\tau_r=2$ ms, an action potential starting out at node one and propagating to node two can backfire to node one if the propagation speed of the action potential u is less than $2\Delta/\tau_r$ where Δ is the distance between the two nodes, i.e., for our model axon $\Delta=350$ μm. Thus backfiring *between two subsequent nodes* is expected to occur if the speed of the action potential is below 0.35 m/s. The speed of the action potential in Fig. 4(a) is approximately 0.7 m/s while it is only 0.35 m/s in Fig. 4(b) with a larger internodal capacitance. Consistent with the simple criteria developed above, backfiring is seen in Fig. 4(b). As described below, this theory is not complete. Other effects than the competition between refractoriness and propagation time are relevant for axonal oscillations.

Next we study the effect of internodal sodium ion channels. At constant values of $g_{\mathrm{leak}_i}=0.005$ mS/cm^2, and $c_{m_i}=0.005$ μF/cm^2, we change the value of g_{Na_i} from 0.5 mS/cm^2 to 3 mS/cm^2. An external current pulse is injected into node one to evoke an action potential there. The subsequent action potentials of node one and node two are plotted in Fig. 5. Increasing the conductance of internodal sodium ion channels, the shape of the action potentials changes suddenly. Below a sodium conductance of $g_{\mathrm{Na}_i}=2$ mS/cm^2, tonic spiking can be observed, below a sodium conductance of $g_{\mathrm{Na}_i}=3$ mS/cm^2, tonic oscillation can be observed. Thus, a relatively large value of internodal sodium conductance in development can induce axonal oscillation when the internodal potassium ion channels are blocked.

Because there are no low-threshold calcium ion channels in the system, the mechanism of the oscillation activity is purely due to backfiring of action potential. Increasing the internodal sodium conductance will enhance the excitability of the internodal membrane, enhance the back propagation of the action potential and thus can facilitate onset of axonal oscillation.

The next question we consider is whether internodal sodium channels are *necessary* for the axonal oscillation. To this end we block all internodal sodium channels, i.e., we set the internodal sodium conductance to zero. In order to guarantee the success of action potential propagation from node one to node two, we increase the axon diameter to 10 μm, and shorten the length of the internode to 250 μm. Increasing the capacitance of the internodal membrane, i.e. reducing the speed of action potential propagation we find axonal oscillation. Thus internodal sodium ion channels are not necessary for axonal oscillation.

By carefully inspecting the sequence of action potentials in Fig. 4 we realize that the qualitative picture of action potentials bouncing back from node two to node one seems to be only correct at the onset of axonal oscillation. In Fig. 4(d) node one fires the second time before node two has ever fired. Furthermore, the period of the oscillations (same figure) is too short for action potential propagation delayed spikes as can be seen by the long time interval between the first spike of node one and the first spike of node two. Thus our hypothesis is that the backfiring can occur through sodium channels in the internode. To this end we remove node two and evoke an action potential in node one.

We delete the second node, evoke action potentials at the remaining node and perform simulations under the same conditions as in Figs. 3–5. In the presence of internodal sodium channels we find—similar as in the case with two nodes (Figs. 3–5)—onset of axonal oscillation with increasing internodal membrane capacitance and sodium channel conductance (see Fig. 6 for the effect of increasing internodal sodium channels). Thus, as hypothesized above, axonal oscillations can be facilitated through backfiring at internodal sodium channels. In the absence of internodal sodium channels, however, no oscillation can be observed in the absence of the second node. Thus, in the absence of internodal sodium channels, only backfiring *between nodes* generates axonal oscillation.

C. The role of internodal potassium ion channels

In order to test the role of internodal potassium ion channels, we set the conductance of potassium ion channels g_{K_i} in juxtaparanodes to 6 mS/cm^2. For the conductance of the internodal sodium channels and internodal membrane capacitance we pick values at which axonal oscillations are observed, i.e., $g_{\mathrm{Na}_i}=0.5$ mS/cm^2, $g_{\mathrm{leak}_i}=0.005$ mS/cm^2, and $c_{m_i}=0.03$ μF/cm^2. In the absence of internodal potassium channels, the axon exhibits oscillation as shown in Fig. 4(d). The action potentials in the presence of internodal potassium ion channels (see Fig. 7) do eliminate axonal oscillation, consistent with the experimental observation in [11]. Thus internodal potassium ion channels stabilize the internodal axolemma against oscillation.

An interesting point is that the required potassium conductance in order to prevent axonal oscillation depends on

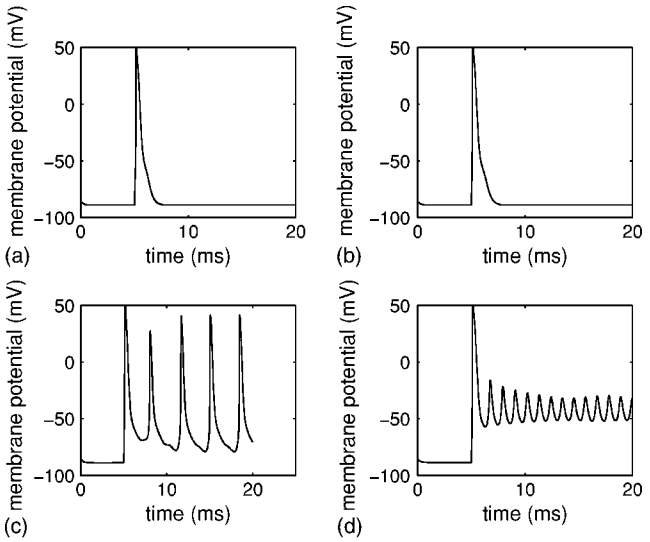

FIG. 6. Action potentials of a single node connected to an internode without juxtaparanodal potassium channels. The solid line depicts the action potentials at the node. An electrical current pulse is injected into the node to evoke an action potential. The parameter values are $g_{\mathrm{leak}_i}=0.005\ \mathrm{mS/cm^2}$, $c_{m_i}=0.005\ \mu\mathrm{F/cm^2}$, $g_{\mathrm{Na}_i}=0.5\ \mathrm{mS/cm^2}$ (a), $g_{\mathrm{Na}_i}=1\ \mathrm{mS/cm^2}$ (b), $g_{\mathrm{Na}_i}=2\ \mathrm{mS/cm^2}$ (c), and $g_{\mathrm{Na}_i}=3\ \mathrm{mS/cm^2}$ (d).

the spatial distribution of these channels. In order to inhibit the oscillation activity for the parameter sets in Fig. 3(d), the conductance of potassium ion channels in juxtaparanodes must be larger than 200 $\mathrm{mS/cm^2}$. Instead, if internodal potassium ion channels are distributed uniformly along the axon, an internodal potassium conductance of as low as 1 $\mathrm{mS/cm^2}$ is sufficient to inhibit the oscillation activity. Thus, a uniform distribution of internodal potassium ion channels is more efficient to inhibit the oscillation activity than a localized juxtaparanodal distribution. On the other hand, the conduction speed is also affected by the distribution of the potassium channels. In general, internodal and juxtaparanodal potassium channels slow down the speed of the action potential of the purely passive cable. Localizing the potassium channels on the juxtaparanodes, however, leaves the internodes almost passive (except some internodal sodium channels) and thus the reduction of the conduction speed is small in comparison to a uniform distribution at the same conductance. In Fig. 8, the effects of internodal potassium channels on action potential propagation speed in two cases are shown. For an internodal membrane capacitance of 0.02 $\mu\mathrm{F/cm^2}$, a maximum internodal sodium conductance of 2.0 $\mathrm{mS/cm^2}$ the propagation speed in the absence of potassium channels is 0.366 m/s. For a maximum internodal potassium channel conductance of 10 $\mathrm{mS/cm^2}$ the conduction speed is 0.249 m/s for a uniform potassium channel distribution, but 0.348 m/s for juxtaparanodal distribution.

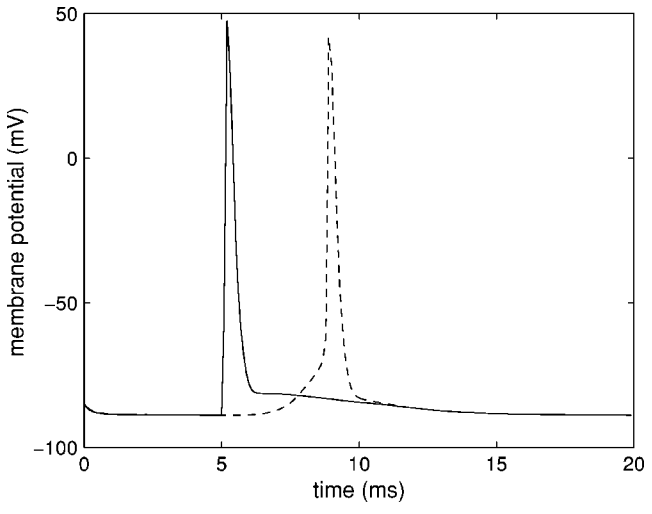

FIG. 7. Action potentials of two connected nodes with juxtaparanodal potassium ion channels. Solid line is the action potential of node one. Dashed line is the action potential of node two. Stimuli current is injected in node one. The parameters are $g_{\mathrm{Na}_i}=0.5\ \mathrm{mS/cm^2}$, $g_{\mathrm{leak}_i}=0.005\ \mathrm{mS/cm^2}$, and $c_{m_i}=0.03\ \mu\mathrm{F/cm^2}$.

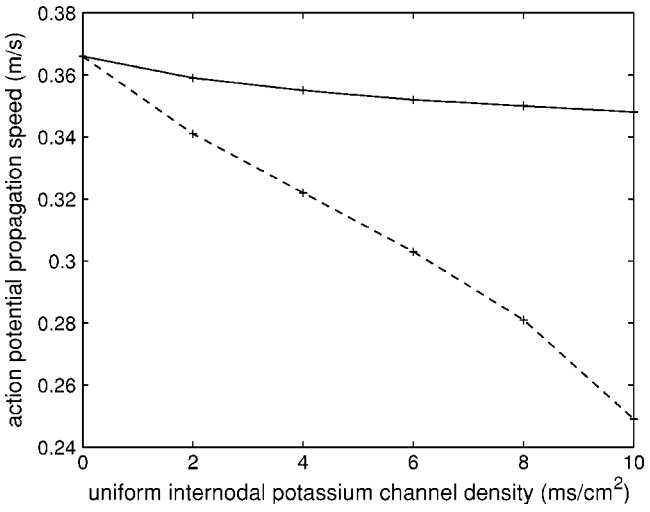

FIG. 8. The effects of internodal potassium channels on action potential propagation speed. The solid line depicts the effect of localized potassium channels in juxtaparanode on action potential propagation speed. The dashed line depicts the effect of uniformly distributed internodal potassium channels on action potential propagation speed. The parameter values are $g_{\mathrm{leak}_i}=0.005\ \mathrm{mS/cm^2}$, $c_{m_i}=0.02\ \mu\mathrm{F/cm^2}$, and $g_{\mathrm{Na}_i}=2\ \mathrm{mS/cm^2}$.

IV. SUMMARY AND CONCLUSIONS

We simulated the action potentials of two nodes connected by an axon. Our simulation results show that blockage of internodal potassium ion channels can induce axonal oscillations in *developing* axons, but has no effect on the action potentials of normal *mature* axons. These results are consistent with the experimental results [9,10]. Our simulation results also show—consistent with experimental results [11]—that internodal potassium ion channels stabilize the internodal axolemma, and prevent axonal oscillation in developing axons. We tested the effects of axonal parameters with respect to onset of axonal oscillation. While the leakage current has no effect on axonal oscillation, increasing internodal sodium conductance as well as increasing internodal membrane capacitance can facilitate axonal oscillation. Increasing

the conductance of internodal sodium ion channels increases the excitability of the axon and therefore also the chance for back-propagation leading to axonal oscillation. Increasing the capacitance of internodal membrane affects axons in two aspects. First, an increasing capacitance leads to a slower propagation speed and thus an increase in the time an action potential takes to propagate between node one and node two or node one and some other internodal active site and back to node one. If this time is large enough, reexcitation of node one leads to backfiring and possibly to persistent axonal oscillations. The other aspect is that it increases the charge carried by the back propagated action potential. We furthermore find that one node connected with an axon is sufficient to induce axonal oscillation if sufficient numbers of sodium channels are present along the axon. In order to investigate the oscillation mechanism, we first chose the simplest model, two nodes connected by an axon. We also simulate the systems with three nodes and four nodes, and get the similarly qualitative result of the system with two nodes.

The mechanism of oscillation, tonic oscillation, tonic spiking described in this paper is facilitated by back propagation of action potentials on the axon. This mechanism is similar to that of oscillation in cortical cells, where the back propagation of action potentials by the dendritic tree causes the oscillation activity [21,22]. But it is different from the mechanism of oscillation in thalamic cells, where the somatic low-threshold calcium current induces the oscillation activity [23,24]. In Pinsky and Rinzel's model [25] for CA3 pyramidal cells, oscillation in their CA3 models is the interaction between the lower threshold, fast, sodium currents in the soma compartment and the higher threshold, slower Ca and Ca dependent currents in the dendrite compartment. In model sensory neuron [26], there is a saddle-node bifurcation of periodic orbits that separates tonic spiking from oscillation. A ping-pong effect that has been described by Pinsky and Rinzel [25] and Laing and Longtin [26] caused by soma-dendrite interaction models by two compartments is similar in appearance to the one we report along the axon in this paper. Different physical properties of the two compartments are the cause for the ping-pong of excitation between soma and dendrites. In our paper, we study axonal dynamics only and find a ping-pong effect along the axon under specified physiological conditions and specified spatial distribution of ion channels.

[1] B. Hille, *Ion Channels of Excitable Membranes* (Sinauer Associates Inc., Sunderland, MA, 2001).
[2] S. Y. Chiu and J. M. Ritchie, J. Physiol. (London) **313**, 415 (1981).
[3] P. Shrager, J. Physiol. (London) **392**, 587 (1987).
[4] P. Shrager, J. Physiol. (London) **404**, 695 (1988).
[5] P. Shrager, Brain Res. **483**, 149 (1989).
[6] S. Y. Chiu, J. M. Ritchie, R. B. Rogart, and D. Stagg, J. Physiol. (London) **292**, 149 (1979).
[7] H. Wang, D. D. Kunkel, T. M. Martin, P. A. Schwartzkroin, and B. L. Tempel, Nature (London) **365**, 75 (1993).
[8] A. L. Hodgkin and A. F. Huxley, J. Physiol. (London) **117**, 500 (1952).
[9] C. M. Bowe, J. D. Kocsis, and S. G. Waxman, Proc. R. Soc. London, Ser. B **224**, 355 (1985).
[10] J. D. Kocsis, S. G. Waxman, C. Hildebrand, and J. A. Ruiz, Proc. R. Soc. London, Ser. B **217**, 77 (1982).
[11] I. Vabnick, J. S. Trimmer, T. L. Schwarz, S. R. Levinson, D. Risal, and P. Shrager, J. Neurosci. **19**, 747 (1999).
[12] S. Y. Chiu and J. M. Ritchie, J. Physiol. (London) **322**, 485 (1982).
[13] S. Y. Chiu and J. M. Ritchie, Proc. R. Soc. London, Ser. B **220**, 415 (1984).
[14] J. Keener and J. Sneyd, *Mathematical Physiology* (Springer-Verlag, Berlin, 2000).
[15] D. H. Perkel and B. Mulloney, Am. J. Physiol. **235**, 93 (1978).
[16] W. Rall, *Neural Theory and Modelling* (Stanford University Press, Stanford, CA, 1964).
[17] P. C. Bressloff, Phys. Rev. E **50**, 2308 (1994).
[18] C. C. Mcintype, A. G. Richardson, and W. M. Grill, J. Neurophysiol. **87**, 995 (2002).
[19] C. Koch, *Biophysics of Computation: Information Processing in Single Neurons* (Oxford University Press, New York, Oxford, 1999).
[20] S. G. Waxman and J. M. Ritchie, Science **228**, 1502 (1985).
[21] D. Franceschetti, E. Guatteo, F. Panzica, G. Sancini, E. Wanke, and G. Avanzini, Brain Res. **696**, 127 (1995).
[22] R. Azouz, M. S. Jensen, and Y. Yaari, J. Physiol. (London) **492**, 211 (1996).
[23] H. Jahnsen and R. Llinas, J. Physiol. (London) **349**, 205 (1984).
[24] W. Guido and T. Weyand, J. Neurophysiol. **74**, 1782 (1995).
[25] P. F. Pinsky and J. Rinzel, J. Comput. Neurosci. **1**, 39 (1994).
[26] C. R. Laing and A. Longtin, Phys. Rev. E **67**, 051928 (2003).